RSC Advances

PAPER

View Article Online
View Journal | View Issue

Cite this: *RSC Adv.*, 2023, **13**, 5168

Proton transfer network with luminescence display controls OFF/ON catalysis that generates a high-speed slider-on-deck†

Sohom Kundu,‡ Isa Valiyev, ‡ Debabrata Mondal, Vishnu Verman Rajasekaran, Abir Goswami and Michael Schmittel *

Received 4th January 2023
Accepted 23rd January 2023

DOI: 10.1039/d3ra00062a

rsc.li/rsc-advances

A three-component network for OFF/ON catalysis was built from a protonated nanoswitch and a luminophore. Its activation by addition of silver(I) triggered the proton-catalyzed formation of a biped and the assembly of a fast slider-on-deck (k_{298} = 540 kHz).

Proton relays in living systems[1] are often coupled to biomachinery with enzymatic catalysis.[2] Frequently, such proton transfer systems comprise intricate networks with information exchange[3,4] amongst multiple components. Using manmade molecules,[5] however, it is still arduous to create networks that approach the complexity[6] and functions of biosystems.

Although activation *via* proton transfer plays an eminent role in molecular logic,[7] switching,[8–10] and machine operation,[11–15] proton transfer networks in combination with the regulation of catalysis remain scarce.[16,17] Beyond that, we present the *in situ* catalytic synthesis of a highly dynamic supramolecular device by a new proton transfer network requiring interference-free information handling,[18] self-sorting[19–21] and communication[22] among multiple components.[23–25]

Recently, our group has developed various chemically actuated networks of communicating components and used them for the ON/OFF regulation of transition metal catalysis.[26–28] Herein, we describe a proton relay system that reversibly toggles between two networked states and is useful for regulation of acid catalysis. It catalyzes an amine deprotection which was utilized to fabricate *in situ* a high-speed slider-on-deck,[29,30] for the first time based on aniline → zinc-porphyrin[31] (N_{an} → ZnPor) interactions.

The communicating network consists of nanoswitch **1** (ref. 32) and luminophore **2** (ref. 33) as receptors (Fig. 1). In the self-sorted networked state (NetState-I), the added proton is captured in the cavity of nanoswitch **1** resulting in $[H(\mathbf{1})]^+$, while luminophore **2** remains free. NetState-I is catalytically inactive as the encapsulated proton is unable to catalyze the deprotection of the trityl protected slider biped **4**. Upon addition of $AgBF_4$ to NetState-I, the silver(I) coordinates to switch **1** and the proton is released onto luminophore **2** thus leading to formation of $[Ag(\mathbf{1})]^+$ and $[H(\mathbf{2})]^+$ in NetState-II (see Scheme 1), which may be followed by characteristic ratiometric emission changes. If NetState-II is formed in presence of **3** and **4**, the catalytic trityl deprotection of **4** produces the free biped **5** that eventually binds to deck **3** furnishing the slider-on-deck $[(\mathbf{3})(\mathbf{5})]$.

The concept of the catalyzed biped formation through a proton transfer network relies on the following considerations: (a) the initial networked state should be catalytically inactive as expected from a self-sorting of the proton inside the nanoswitch leaving the luminophore free. (b) Addition of silver(I) ions should release the proton from the protonated switch thus forming the protonated luminophore which we anticipated to act as catalyst. (c) A di-protected biped should undergo acid catalyzed deprotection by the protonated luminophore and eventually form a slider-on-deck by coordination to a deck. (d)

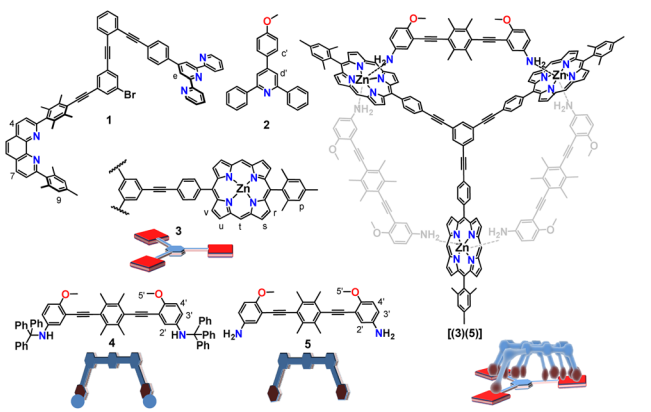

Fig. 1 Chemical structures and cartoon representations of the ligands used in the study.

Center of Micro and Nanochemistry and (Bio)Technology, Organische Chemie I, Universität Siegen, Adolf-Reichwein-Str. 2, D-57068 Siegen, Germany. E-mail: schmittel@chemie.uni-siegen.de; Tel: +49 2717404356

† Electronic supplementary information (ESI) available: Experimental procedures, compound characterizations, spectral data, UV-vis titrations and computational data. See DOI: https://doi.org/10.1039/d3ra00062a

‡ Sohom Kundu and Isa Valiyev contributed equally.

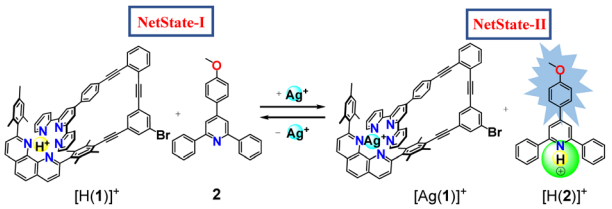

Scheme 1 Schematic representation of the reversible proton relay network. Green circle represents catalytic site.

Finally, the product of the catalysis should not intervene in any state of the operation with the main system.

As proton receptor we chose the known phenanthroline–terpyridine nanoswitch **1** (ref. 32) in order to tightly capture the proton/silver(I) as HETTAP (HETeroleptic Terpyridine And Phenanthroline) complexes.[34] Luminophore **2** was based on the 2,4,6-triarylpyridine scaffold which is known to fluoresce strongly upon protonation due to intramolecular charge transfer (ICT).[35]

To investigate the self-sorting within the network, we mixed nanoswitch **1**, luminophore **2** and TFA in 1 : 1 : 1 ratio in CD_2Cl_2 which furnished NetState-I = $[H(\mathbf{1})]^+$ + **2**. ^{1}H NMR shifts of the 4/7-H proton signals to 8.43 and 8.69 ppm and of 9-H and e-H proton peaks to 6.60 and 8.48 ppm confirmed formation of $[H(\mathbf{1})]^+$. Moreover, proton signals of c′-H and d′-H at 7.07 and 7.92 ppm corroborated presence of the free luminophore **2** (Fig. 2). Addition of one equiv. of $AgBF_4$ to NetState-I instantaneously generated NetState-II = $[Ag(\mathbf{1})]^+$ + $[H(\mathbf{2})]^+$. In the ^{1}H NMR of NetState-II, the 9-H and e-H proton signals shifted to 6.55 and 8.23 ppm, respectively, which substantiated the formation of $[Ag(\mathbf{1})]^+$ whereas the shift of proton peaks c′-H and d′-H to 7.12 and 8.00 ppm, respectively, established the protonated luminophore $[H(\mathbf{2})]^+$ (Fig. 2). Upon excitation at 300 nm, NetState-I exhibited emissions at λ = 346, 372 and 393 nm which represent an overlap of the emission peaks of the free luminophore **2** at λ = 346 and 372 nm and of $[H(\mathbf{1})]^+$ at λ = 376 and 393 nm (Fig. 3c). In NetState-II, the fluorescence spectrum showed a single emission at λ = 461 nm, which is attributed to $[H(\mathbf{2})]^+$ (Fig. 3). In contrast, $[Ag(\mathbf{1})]^+$ in NetState-II is nonfluorescent as advocated by the full quenching of the emission of $[H(\mathbf{1})]^+$ at λ = 376 and 393 nm upon titration with silver(I) ions (ESI, Fig. S18†). When one equiv. of tetra-*n*-butylammonium iodide (TBAI) was added to NetState-II, complete restoration of NetState-I was achieved as confirmed from ^{1}H NMR data. TBAI acted as a scavenger for silver(I) by removing AgI through precipitation thus reversing the translocation sequence. Multiple switching of NetState-I ⇆ NetState-II was readily followed by ^{1}H NMR (Fig. 2) and luminescence changes. Upon successive addition of $AgBF_4$ to NetState-I, the emission changed to λ = 461 nm (sky blue emission of $[H(\mathbf{2})]^+$) in NetState-II (Fig. 3a and b) in a clean ratiometric manner that allowed monitoring of the amount of liberated protons. Alternating switching between the NetStates was followed by emission spectroscopy over three cycles with a small decline in emission intensity (Fig. 3c and d), which may be due to the progressive accumulation of AgI.

For probing the catalytic efficiency of each state towards a simple amine deprotection reaction we chose the trityl-protected aniline **6** (Fig. 4) performing two NetState-I ⇆ NetState-II cycles (Fig. 4b). We first prepared NetState-I by mixing **1**, **2** and TFA (1 : 1 : 1) in CD_2Cl_2 and then added **6** and TMB (1,3,5-trimethoxybenzene as an internal standard) in a 10 : 10 ratio. After heating for 2 h at 40 °C, the ^{1}H NMR spectrum revealed no product **7**. Clearly, the proton in $[H(\mathbf{1})]^+$ is catalytically inactive (ESI, Fig. S10b†). Addition of one equiv. of $AgBF_4$ and probing the catalysis again for 2 h at 40 °C revealed formation of product **7** in (30 ± 2)% yield (ESI, Fig. S10c†). When the catalytic experiment was probed with only $[H(\mathbf{2})]^+$

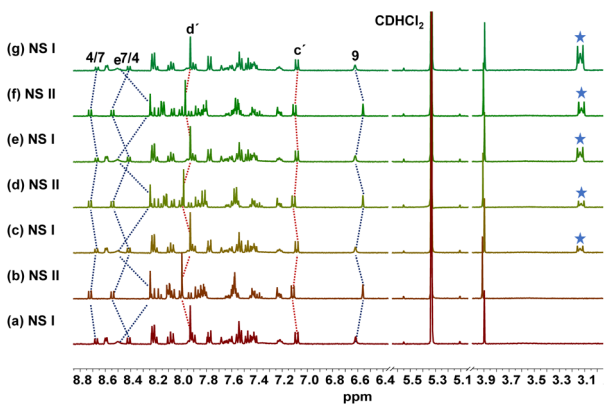

Fig. 2 Partial ^{1}H NMR spectra (500 MHz, CD_2Cl_2, 298 K) showing reliable switching between NetState-I and II over 3 cycles. (a) After mixing of TFA, **1**, and **2** in 1 : 1 : 1 ratio; (b) after adding 1.0 equiv. of $AgBF_4$ furnishing $[Ag(\mathbf{1})]^+$ and $[H(\mathbf{2})]^+$; (c) after addition of 1.0 equiv. of TBAI; (d) after adding 1.0 equiv. of $AgBF_4$; (e) after addition of 1.0 equiv. of TBAI, (f) after adding 1.0 equiv. of $AgBF_4$; (g) after addition of 1.0 equiv. of TBAI. Blue asterisk marked proton signals represent the tetrabutylammonium ion.

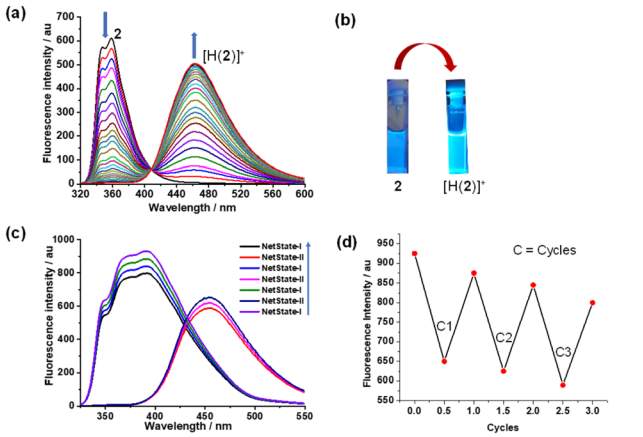

Fig. 3 (a) Ratiometric emission titration of **2** (2.1×10^{-5} M) with TFA (5.3×10^{-3} M) in CH_2Cl_2. (b) Change of emission upon protonation of **2**. (c) Reversibility of the network NetState-I ⇆ II over three cycles upon addition of silver(I) and TBAI (see text, blue arrow assigns direction of switching) monitored by luminescence changes at λ = 461 nm. (d) Multiple cycles monitored by the change of the fluorescence intensity.

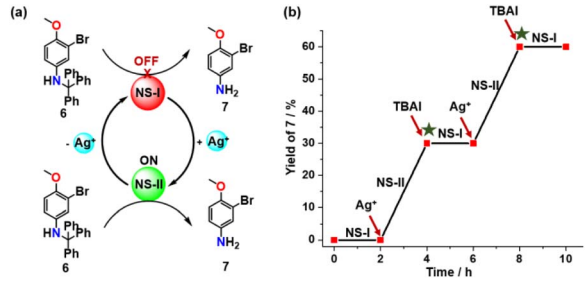

Fig. 4 (a) Representation of the OFF/ON regulation of the trityl deprotection reaction in NetState-I and II. (b) Reversible switching between the network states furnished reproducible amounts of product **7** in NetState-II (two independent runs). Consumed amounts of substrates were added (green asterisk).

under identical reaction conditions, it provided the same yield (ESI, Fig. S16†). This suggested that the reversible proton relay network (Scheme 1) functioned reliably also in presence of **6** with complex $[H(\mathbf{2})]^+$ as the catalytically active species. Addition of one equiv. of TBAI to the above NetState-II mixture and probing for catalysis, revealed no further product formation. Apparently, addition of TBAI translocated back the proton to nanoswitch **1** thus restoring NetState-I, which resulted in the OFF state for catalysis. Adding one equiv. of $AgBF_4$ to the mixture and probing again the catalytic activity resulted in formation of further (29 ± 2)% of product **7**, which was basically identical to the yield produced in the first cycle of NetState-II (ESI, Fig. S10e†). Adding TBAI and the consumed amount of substrate showed no further deprotection. In sum, the robust catalytic performance of the proton relay network as reflected in two successive catalytic cycles resulted in no significant decline of the catalytic activity (Fig. 4b).

The OFF–ON switching of the catalytic trityl deprotection of aniline **6** by the proton relay network inspired us to utilize the system to catalytically fabricate a slider-on-deck based on the N_{an} (= aniline) → ZnPor interaction. Deprotection of the protected biped **4** should afford the bis-aniline biped **5** and enable its attachment to the tris-zinc porphyrin deck **3** thus forming the slider-on-deck [(**3**)(**5**)].

Addition of one equiv. of biped **5** (for synthesis and characterization, see ESI†) to deck **3** (ref. 25) in CD_2Cl_2 quantitatively generated the slider-on-deck [(**3**)(**5**)], which was unambiguously characterized by ^{1}H NMR, ^{1}H DOSY NMR and elemental analysis (ESI, Fig. S5 and S6†). In the ^{1}H NMR-spectrum, several diagnostic shifts of biped and deck proton signals attested the binding of biped **5** to the deck. Formation of the slider-on-deck was further confirmed from a single set in the ^{1}H DOSY in CD_2Cl_2 (ESI, Fig. S9†).

The single set of protons (p-H, r-H, s-H, t-H, u-H, v-H) in the ^{1}H NMR spectrum for all three-zinc porphyrin (ZnPor) stations of deck **3** unmistakably suggested rapid intrasupramolecular exchange[29a] of the aniline biped across all three ZnPor sites requiring fast N_{an} → ZnPor bond cleavage. At low temperature (−65 °C) the ZnPor p-H proton signals separated into two sets (1 : 2) (ESI, Fig. S7 and S8†). Kinetic analysis over a wide temperature range provided the exchange frequency (k) with $k_{298} = 540$ kHz at 298 K (Fig. 5a) and the activation data as $\Delta H^{\ddagger} = 41.5 \pm 0.7$ kJ mol^{-1}, $\Delta S^{\ddagger} = 2.8 \pm 0.7$ J mol^{-1} K^{-1} and $\Delta G^{\ddagger}_{298} = 40.7$ kJ mol^{-1} (Fig. 5).

After determining the kinetic parameters of the slider-on-deck [(**3**)(**5**)], we investigated its *in situ* catalyzed formation by the proton relay network. Therefore, we mixed nanoswitch **1**, luminophore **2**, TFA, trityl-protected biped **4**, deck **3** and TMB in 1 : 1 : 1 : 5 : 5 : 5 ratio in CD_2Cl_2 and heated the reaction mixture for 12 h at 40 °C. The ^{1}H NMR spectrum suggested no formation of any slider-on-deck in NetState-I (ESI, Fig. S13†). Addition of one equiv. of $AgBF_4$ to the same mixture (converting NetState-I to NetState-II) and heating it at 40 °C for 12 h revealed full formation of the slider-on-deck as indicated by the disappearance of the 2′-H, 3′-H and 4′-H proton signals of biped **4** at 6.60, 6.31 and 6.51 ppm (ESI, Fig. S11†), respectively, and the quantitative emergence of 4′-H proton signal of biped **5** bound to deck **3** at 5.84 ppm (ESI, Fig. S12†). The upfield shift of the deck's *meso* t-H protons from 10.36 to 10.29 ppm allowed monitoring of the formation of [(**3**)(**5**)], *e.g.* by the gradually increased chemical shift difference of proton signal t-H ($\Delta\delta_{t\text{-}H}$) (Fig. 6a; ESI, Fig. S11†). In sum, the protonated $[H(\mathbf{2})]^+$ in NetState-II catalyzed the deprotection of the trityl-protected biped **4** with the effect that the resultant bis-aniline biped **5** would quantitatively bind to deck **3** affording the slider-on-deck [(**3**)(**5**)]. Furthermore, the OFF/ON switching of catalysis was probed for shortened time periods of 3 h. As illustrated in Fig. 6b, the process could be readily followed using the proton signal t-H ($\Delta\delta_{t\text{-}H}$) (ESI, Fig. S14†) and the growth of proton signal 4′-H at 5.84 ppm of bound biped **5** (ESI, Fig. S15†). One clearly sees recurring OFF/ON regulation in NetState-I/II.

In conclusion, we have designed a supramolecular multicomponent network[36] that acts as an OFF/ON proton relay with a luminescence display[37] and is useful for switchable catalysis.[38] The network is toggled by chemical input and intercomponent communication[15,16] and as a result is a conceptual complement to photoacids driving networks.[7,8]

The release and capture of protons is demonstrated by the ON/OFF trityl deprotection of anilines. To demonstrate functioning in a complex setting, the network was utilized to catalyze formation of a high-speed slider-on-deck assembly based on N_{an} → ZnPor interactions (sliding frequency of k_{298} = 540 kHz). The robust operation of the proton relay furnishing dynamic machinery[39]

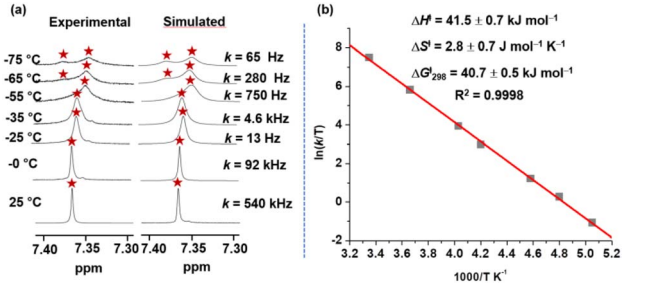

Fig. 5 (a) Experimental and theoretical splitting of p-H proton signal of nanoslider [(**3**)(**5**)] in VT ^{1}H-NMR (600 MHz) furnishing rate data in CD_2Cl_2. (b) Eyring plot providing kinetic parameters.

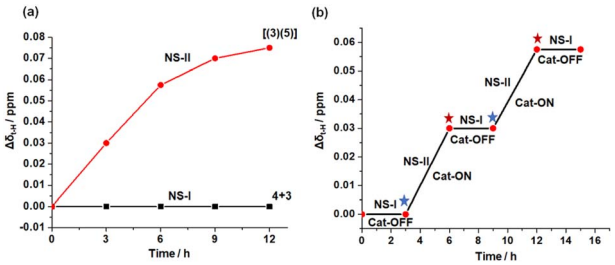

Fig. 6 Plot of the shift difference of proton signal t-H ($\Delta\delta_{t\text{-}H}$) *vs.* time for (a) the formation of [(3)(5)] from 3 and 4. Red curve: formation of [(3)(5)] over 12 h catalyzed by NetState-II. Black curve: OFF state of catalysis in NetState-I. (b) OFF/ON catalytic cycles by switching between NetState-I and NetState-II. Addition of Ag^+, see blue asterisk; addition of TBAI: red asterisk.

through acid catalysis followed by self-assembly is a valuable step mimicking sophisticated biological proton relays.[2]

Conflicts of interest

There are no conflicts to declare.

Acknowledgements

We are indebted to the Deutsche Forschungsgemeinschaft for continued support under Schm 647/22-1 (No. 491092614) and to the University of Siegen. We thank Dr Paululat (Siegen) for measuring the VT-^{1}H NMR.

Notes and references

1 D. Ray, J. T. Foy, R. P. Hughes and I. Aprahamian, *Nat. Chem.*, 2012, **4**, 757–762.
2 T. R. Li, F. Huck, G. M. Piccini and K. Tiefenbacher, *Nat. Chem.*, 2022, **14**, 985–994.
3 M. Schmittel and P. Howlader, *Chem. Rec.*, 2021, **21**, 523–554.
4 J. Andréasson and U. Pischel, *Coord. Chem. Rev.*, 2021, **429**, 213695.
5 F. R. Ludlow and S. Otto, *Chem. Soc. Rev.*, 2008, **37**, 101–108.
6 J. L. Dempsey, J. R. Winkler and H. B. Gray, Proton-coupled electron flow in protein redox machines, *Chem. Rev.*, 2010, **110**, 7024–7039.
7 S. Silvi, E. C. Constable, C. E. Housecroft, J. E. Beves, E. L. Dunphy, M. Tomasulo, F. M. Raymo and A. Credi, *Chem.–Eur. J.*, 2009, **15**, 178–185.
8 F. M. Raymo and S. Giordani, *Org. Lett.*, 2001, **3**, 3475–3478.
9 M. Kadarkaraisamy, G. Caple, A. R. Gorden, M. A. Squire and A. G. Sykes, *Inorg. Chem.*, 2008, **47**, 11644–11655.
10 S. Yang, C.-X. Zhao, S. Crespi, X. Li, Q. Zhang, Z.-Y. Zhang, J. Mei, H. Tian and D.-H. Qu, *Chem*, 2021, **7**, 1544–1556.
11 J. A. Findlay and J. D. Crowley, *Tetrahedron Lett.*, 2018, **59**, 334–346.
12 A. W. Heard and S. M. Goldup, *ACS Cent. Sci.*, 2020, **6**, 117–128.
13 S. Krause and B. L. Feringa, *Nat. Rev. Chem.*, 2020, **4**, 550–562.
14 S. Amano, S. Borsley, D. A. Leigh and Z. Sun, *Nat. Nanotechnol.*, 2021, **16**, 1057–1067.
15 M. N. Tasbas, E. Sahin and S. Erbas-Cakmak, *Coord. Chem. Rev.*, 2021, **443**, 214039.
16 J. T. Foy, D. Ray and I. Aprahamian, *Chem. Sci.*, 2015, **6**, 209–213.
17 S. Pramanik and I. Aprahamian, *J. Am. Chem. Soc.*, 2017, **138**, 15142–15145.
18 Q. Wang, B. Lin, M. Chen, C. Zhao, H. Tian and D.-H. Qu, *Nat. Commun.*, 2022, **13**, 4185.
19 W. M. Bloch and G. H. Clever, *Chem. Commun.*, 2017, **53**, 8506–8516.
20 S. Gaikwad, M. S. Özer, S. Pramanik and M. Schmittel, *Org. Biomol. Chem.*, 2019, **17**, 7956–7963.
21 J.-F. Ayme, S. Dhers and J.-M. Lehn, *Angew. Chem., Int. Ed.*, 2020, **59**, 12484–12492.
22 P. Remon and U. Pischel, *ChemPhysChem*, 2017, **18**, 1667–1677.
23 P. Remón, D. González, A. M. Romero, N. Basílio and U. Pischel, *Chem. Commun.*, 2020, **56**, 3737–3740.
24 S. M. Wales, D. T. J. Morris and J. Clayden, *J. Am. Chem. Soc.*, 2022, **144**, 2841–2846.
25 S. Kundu, A. Ghosh, I. Paul and M. Schmittel, *J. Am. Chem. Soc.*, 2022, **144**, 13039–13043.
26 S. De, S. Pramanik and M. Schmittel, *Angew. Chem., Int. Ed.*, 2014, **53**, 14255–14259.
27 N. Mittal, S. Pramanik, I. Paul, S. De and M. Schmittel, *J. Am. Chem. Soc.*, 2017, **139**, 4270–4273.
28 A. Goswami, T. Paululat and M. Schmittel, *J. Am. Chem. Soc.*, 2019, **141**, 15656–15663.
29 (*a*) I. Paul, A. Goswami, N. Mittal and M. Schmittel, *Angew. Chem., Int. Ed.*, 2018, **57**, 354–358; (*b*) D. Mondal, A. Ghosh, I. Paul and M. Schmittel, *Org. Lett.*, 2022, **24**, 69–73.
30 S. Saha, P. K. Biswas, I. Paul and M. Schmittel, *Chem. Commun.*, 2019, **55**, 14733–14736.
31 M. Tanasova, Q. Yang, C. C. Olmsted, C. Vasileiou, X. Li, M. Anyika and B. Borhan, *Eur. J. Org. Chem.*, 2009, **25**, 4242–4253.
32 A. Goswami, S. Saha, E. Elramadi, A. Ghosh and M. Schmittel, *J. Am. Chem. Soc.*, 2021, **143**, 14926–14935.
33 Z.-H. Ren, Z.-Y. Zhang, B.-Q. Yang, Y.-Y. Wang and Z.-H. Guan, *Org. Lett.*, 2011, **13**, 5394–5397.
34 S. Kundu, D. Mondal, V. V. Rajasekaran, A. Goswami and M. Schmittel, *Inorg. Chem.*, 2022, **61**, 17007–17011.
35 Y. Liu, M. Han, H.-Y. Zhang, L.-X. Yang and W. Jiang, *Org. Lett.*, 2008, **10**, 2873–2876.
36 G. Olivo, G. Capocasa, D. Del Giudice, O. Lanzalunga and S. Di Stefano, *Chem. Soc. Rev.*, 2021, **50**, 7681–7724.
37 E. Spatola, F. Rispoli, D. Del Giudice, R. Cacciapaglia, A. Casnati, L. Marchiò, L. Baldini and S. Di Stefano, *Org. Biomol. Chem.*, 2022, **20**, 132–138.
38 (*a*) L. van Dijk, M. J. Tilby, R. Szpera, O. A. Smith, H. A. P. Bunce and S. P. Fletcher, *Nat. Rev. Chem.*, 2018, **2**, 117; (*b*) R. Parella, S. Jakkampudi, P. Bora, N. Sakkani and J. C.-G. Zhao, *Org. Biomol. Chem.*, 2021, **20**, 163–172.
39 H. Inami, Y. Inagaki and W. Setaka, *Org. Biomol. Chem.*, 2022, **20**, 7092–7098.